

# Nd-Doped TiO<sub>2</sub> Nanorods: Preparation and Application in Dye-Sensitized Solar Cells

Qiaohong Yao, Junfeng Liu, Qing Peng,\* Xun Wang, and Yadong Li<sup>[a]</sup>

**Abstract:** Monodispersed Nd-doped TiO<sub>2</sub> nanorods (20 nm × 2 nm) were synthesized by solvothermal methods and characterized by TEM, XRD, and EDS. Application of the nanorods for modifying conventional photoanodes in dye-sensitized solar cells (DSSCs) was investigated. Data show that, after modification, an enhancement of the

incident-photon-to-current conversion efficiency (IPCE) in the whole range of visible light was observed and an in-

**Keywords:** dyes • solar cells • monodispersed nanoparticles • nanostructures • neodymium • titanium dioxide

crease of 33.3 % for overall conversion efficiency was achieved. Our mechanistic proposal is that Nd ions doped on TiO<sub>2</sub> nanorods to some extent enhance the injection of excited electrons and decrease the recombination rate of the injected electrons.

## Introduction

Dye-sensitized solar cells (DSSCs) that exhibit energy-conversion efficiencies of more than 10 % have been investigated intensively as a cost-effective alternative to conventional solar cells.<sup>[1,2]</sup> In DSSCs, TiO<sub>2</sub> films with mesoscopic texture have been widely used as the photoanode onto which dye sensitizers were adsorbed. Under illumination, excited dye molecules inject electrons into the conduction band of the semiconductor. Injected electrons are then transported to the conducting glass substrate, which is beneficial to the performance of the solar cells. On the other hand, the injected electrons might recombine with the oxidized species in the electrolyte, which is one of the major factors that limit the efficiency of the solar cells.

The photoanode in dye-sensitized solar cells are usually fabricated from a random assembly of anatase nanocrystals.<sup>[3,4]</sup> The synthesis of structures with higher degrees of order than randomly oriented networks is expected, and films with mesoporous channels aligned parallel to each other and vertically with respect to the conducting glass substrate are desired. This facilitates pore diffusion, gives easier access to the film surface, and allows the junction to be

formed under better control.<sup>[4]</sup> Recently, two groups reported highly efficient photoanodes, which were prepared from organized mesoporous TiO<sub>2</sub> films.<sup>[5,6]</sup> These films have larger surface areas and/or higher crystallinity. The 1- $\mu$ m-thick mesoporous films showed an enhanced solar-cell conversion efficiency of about 50 % relative to that of traditional films of the same thickness made from randomly oriented anatase nanocrystals.<sup>[5]</sup> Furthermore, electron transport in crystalline wires is expected to be several orders of magnitude faster than percolation through a random polycrystalline network, hence replacing the nanoparticle film with an array of oriented single-crystalline nanowires was investigated.<sup>[7]</sup> Unfortunately, the efficiency was limited because of the small surface area of the nanowires.<sup>[5,7]</sup>

Modification of titania electrodes by dipping in solutions of various metal compounds followed by calcination is a frequently employed method.<sup>[8–19]</sup> The modified electrodes are thus coated with a thin layer of the metal oxide, which forms an inherent energy barrier at the electrode–electrolyte interface. This barrier decreases the recombination rate of the photoinjected electrons with their counterholes, hence improving the efficiency of the solar cell.<sup>[9,12]</sup> This modification was also shown to improve the dye adsorption and increase the volume of the optically active component, leading to improved cell performance.<sup>[9,10]</sup>

Replacing the entire nanoparticle film with an array of oriented single-crystalline nanowires or nanorods is not realistic. On the other hand, introducing lanthanide into the photoanode of the DSSC would be of great significance because of the possible novel properties induced by their

[a] Q. Yao, J. Liu, Q. Peng, X. Wang, Y. Li  
Department of Chemistry  
Tsinghua University  
Beijing 100084 (China)  
Fax: (+86)10-6278-8765  
E-mail: pengqing@tsinghua.edu.cn

unique electronic structures and the numerous transition modes involving the 4f shell of their ions.

Herein we describe the synthesis of highly crystalline, nearly monodisperse Nd-doped TiO<sub>2</sub> nanorods in well-controlled solvothermal reactions<sup>[20,21]</sup> and the incorporation of the nanorods into conventional TiO<sub>2</sub> photoanodes in DSSCs. This modification is different from the method in which dipping is followed by calcination. Modification of the porous photoelectrode with nanorods did not form a layer of nanorods at the electrode–electrolyte interface, and the probable case is that the nanorods were embedded partly in the pores of the films. It was expected that the simultaneous introduction of lanthanide ions and nanorods would bring about a positive effect on the injection rate of the excited electrons and the transport rate of the injected electrons in the photoanode.

## Results and Discussion

Figure 1 a shows a TEM image of the Nd-doped TiO<sub>2</sub> nanorods. It is easy to see from Figure 1 that the nanorods display uniform morphologies with diameters of 20 nm × 2 nm. The crystalline phases of the Nd-doped TiO<sub>2</sub> nanorods were investigated by using X-ray diffraction (XRD), and the diffraction pattern is depicted in Figure 1 b, in which the reflections were attributed to TiO<sub>2</sub> with anatase structure. No reflections of neodymium oxides were found in the XRD pattern, indicating that Nd atoms were evenly dispersed in the TiO<sub>2</sub> and did not form any crystalline structure. The composition of the nanorods was determined by using energy-dispersive X-ray spectroscopy (EDS), which proved the presence of Nd atoms in the TiO<sub>2</sub> nanorods (Figure 1 c), thus indicating that the doping is successful. Figure 2 shows the scanning electron microscopy (SEM) images of the TiO<sub>2</sub> electrodes before and after modification. It is clearly seen that after modification the surface of the TiO<sub>2</sub> electrode changed substantially. First, the surface of the electrode was interspersed with conglomerations of Nd-doped TiO<sub>2</sub> nanorods. Circles 1 and 2 show examples of the conglomerations, whereas in the area indicated by the arrow one can see structures resembling needles, which should be the nanorods used to modify the electrode. Considering the diameters of the nanoparticles (about 15 nm) in the films and the nanorods (20 nm × 2 nm) investigated in this work, we can understand that the majority of the nanorods were embedded

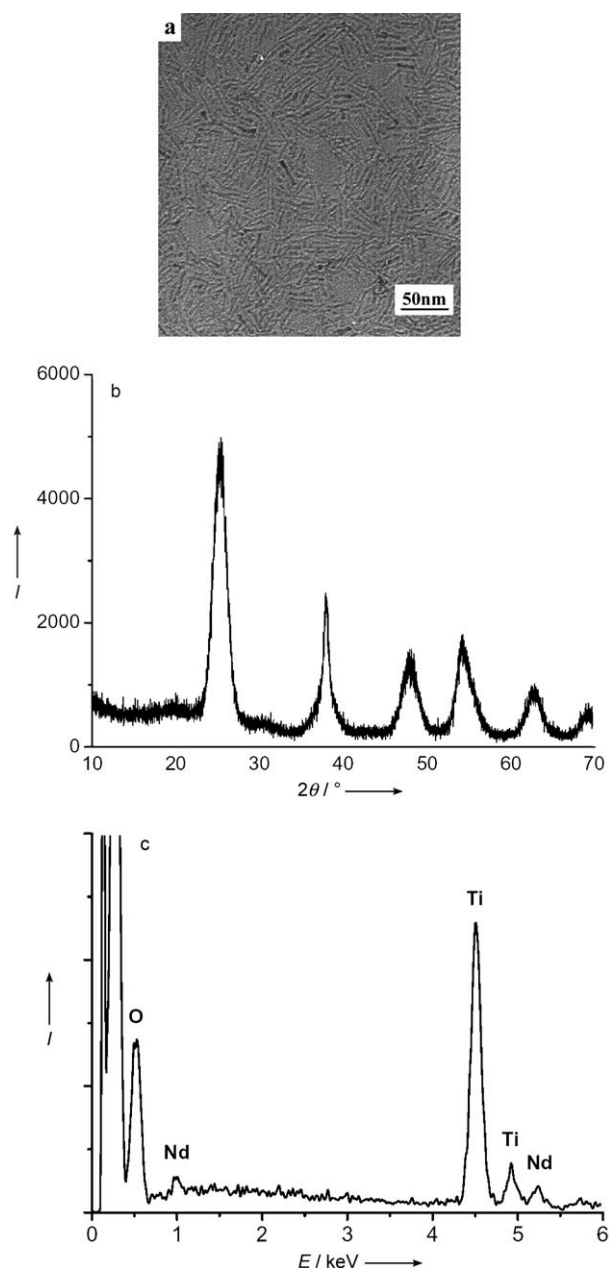


Figure 1. a) TEM image, b) XRD pattern, and c) EDS spectrum of Nd-doped TiO<sub>2</sub> nanorods.

in the small pores of the TiO<sub>2</sub> films. This kind of modification would bring some effect to the specific surface area of the films. This idea could be further confirmed through measuring the absorption spectra of Ru dye N719 (Solaronix) sensitized unmodified and modified electrodes.

The absorption spectra of the two types of electrodes in both bare and dye-sensitized states are presented in Figure 3. Modification with the rods did not dramatically affect the absorption of the TiO<sub>2</sub> films (spectra 1 and 2 in Figure 3), but a red shift of the absorption edge toward the visible region is observed for the modified electrode. This phenomenon is consistent with previous reports<sup>[23]</sup> and could be used as circumstantial evidence for the presence of Nd

### Abstract in Chinese:

利用溶剂热反应合成了单分散的Nd掺杂的TiO<sub>2</sub> (20 nm × 2 nm) 纳米棒, 并用TEM, XRD, 和EDS对纳米棒进行了表征。研究了该纳米棒对染料敏化太阳能电池中的传统光阳极的修饰作用, 结果显示修饰以后电池的IPCE在整个可见光区都有很大提高, 从而使电池的总能量转化效率提高了33.3%。论文提出了该修饰方法改善电池光电性能的可能机理。

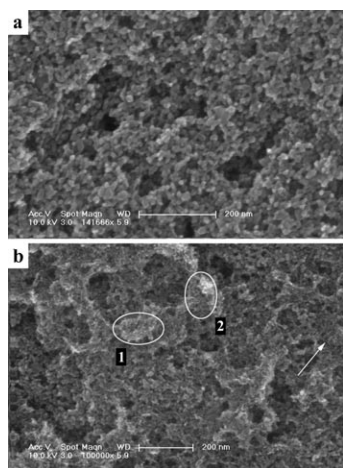


Figure 2. SEM images of TiO<sub>2</sub> films (a) unmodified; b) modified). The actual size of each image is 300 × 300 nm<sup>2</sup>.

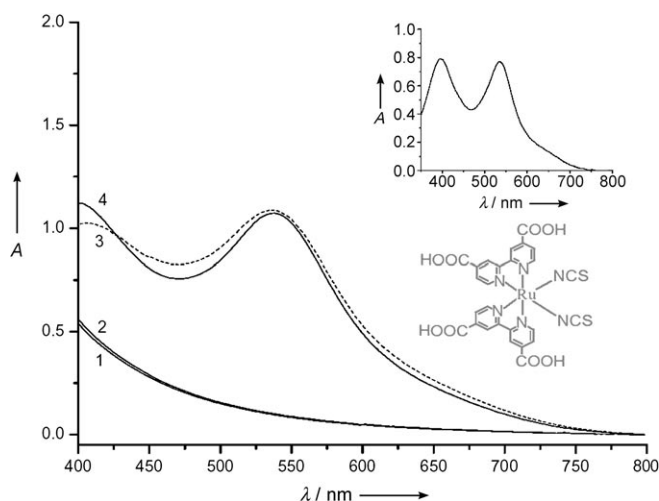


Figure 3. Absorption spectra of 1) unmodified electrode, 2) modified electrode, 3) dye-loaded unmodified electrode, and 4) dye-loaded modified electrode. Inset: structure of the dye and absorption spectrum of the dye/ethanol solution.

atoms in the modified electrode. In the report, the band gap of the TiO<sub>2</sub> nanoparticles was successfully decreased by Nd<sup>3+</sup> doping, and the maximum band gap reduction was 0.55 eV for 1.5 atom % Nd-doped TiO<sub>2</sub> nanoparticles. The decreased band gap was primarily attributed to the substituted Nd<sup>3+</sup> ions, which introduced electron states into the band gap of TiO<sub>2</sub> to form the new lowest unoccupied molecular orbital.<sup>[23]</sup> In our investigation, although the doping level for the nanorods is 5 atom %, the value for the modified electrode would be very small, which consequently results in the very similar absorption spectra of the two unsensitized electrodes.

The absorption spectra for N719 on the two electrodes are almost the same (spectra 3 and 4 in Figure 3), and both spectra are similar in shape to those of the UV/Vis absorption spectrum of a solution of the Ru dye in ethanol. To

clarify the effect of the modification on the adsorption property of the dye, the dyes adsorbed on the TiO<sub>2</sub> films were dissolved completely from the TiO<sub>2</sub> films into a 0.1 M aqueous solution of sodium hydroxide, and the adsorption amount was measured. Values of  $2.3 \times 10^{-8} \text{ mol cm}^{-2}$  and  $2.2 \times 10^{-8} \text{ mol cm}^{-2}$  were obtained for the unmodified and modified electrodes, respectively. The value for the modified electrode is negligibly lower than that of the unmodified electrode, thus showing that the amount of N719 adsorbed on TiO<sub>2</sub> films was also not dramatically affected by the modification.

Short-circuit photocurrents were measured at various excitation wavelengths for an unmodified solar cell (based on an unmodified electrode) and a modified solar cell (based on a modified electrode), and the monochromatic incident photon-to-electron conversion efficiency (IPCE), defined as the number of electrons generated by light in the outer circuit divided by the number of incident photons, was obtained by Equation 1:

$$\text{IPCE}(\%) = \frac{1240 I_{\text{sc}} (\mu\text{A cm}^{-2})}{\lambda (\text{nm}) P_{\text{in}} (\text{W m}^{-2})}$$

where the constant 1240 is derived from the units of conversion,  $I_{\text{sc}}$  is the short-circuit photocurrent generated by monochromatic light, and  $\lambda$  is the wavelength of the incident monochromatic light of intensity  $P_{\text{in}}$ . The photocurrent action spectra (Figure 4a) represent the IPCE versus incident light of various wavelengths. The IPCE values of the modified solar cell, in the whole photosensitization region from 400 nm to 800 nm, are higher than those for the unmodified solar cell. The increase percentage of IPCE has a minimum value of about 19% at 500, 520, and 540 nm, and shows maximum values of 24% at 400 nm and 30% at 800 nm. The increase indicates that modified solar cells have a higher electron-injection efficiency and/or collection efficiency of injected electrons than the unmodified cells, showing that the modified solar cell would have better photoelectrochemical properties.

The photoelectrochemical properties of the solar cells are given in Table 1, and the photocurrent–voltage curves are shown in Figure 4b. The fill factor (FF) is given by Equation 2:

$$\text{FF} = (V_{\text{opt}} I_{\text{opt}}) / (V_{\text{oc}} I_{\text{sc}})$$

where  $V_{\text{opt}}$  and  $I_{\text{opt}}$  are the voltage and the current for maximum power output, respectively, and  $V_{\text{oc}}$  and  $I_{\text{sc}}$  are the open-circuit photovoltage and the short-circuit photocurrent, respectively. The overall yield ( $\eta$ ) is expressed by Equation 3:

$$\eta = (V_{\text{oc}} I_{\text{sc}} \text{FF}) / P_{\text{in}}$$

where  $P_{\text{in}}$  is the power of the incident white light. In this case, the power of the incident white light is  $84.0 \text{ mW cm}^{-2}$ . Consistent with our analysis from the action spectrum, the

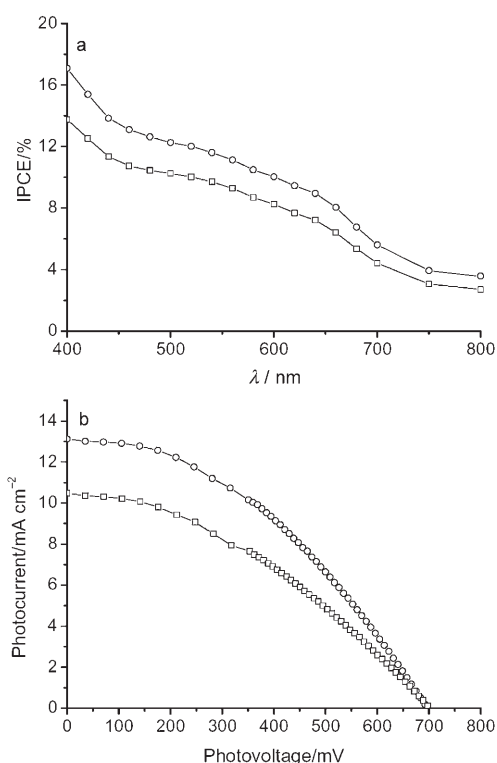


Figure 4. a) Action spectra and b) current–voltage curves of DSSCs. ○ = Modified, □ = unmodified.

Table 1. Parameters of DSSCs based on different electrodes.

	$I_{sc}$ [ $\text{mA cm}^{-2}$ ]	$V_{oc}$ [mV]	FF	$\eta$ [%]
modified	13.1	701	0.401	4.4
unmodified	10.7	707	0.366	3.3

modified solar cell generated a higher light-to-electricity efficiency of 4.4% ( $I_{sc}=13.1 \text{ mA cm}^{-2}$ ,  $V_{oc}=701 \text{ mV}$ , FF=0.401). Relative to the unmodified solar cell, the energy conversion increased by 33.3%, the short-circuit photocurrent increased by 22.4%, the fill factor by 9.6%, and the open-circuit photovoltage exhibited a small change of 6 mV.

It is understood that coating the mesoporous oxide films in DSSCs with a very thin conformal overlayer of an insulator can increase the open-circuit photovoltage, hence improving the efficiency of DSSCs.<sup>[15]</sup> In other cases, the coating forms an inherent energy barrier at the electrode–electrolyte interface, thus decreasing the recombination rate of the injected electrons with their counterholes and improving the parameters of the solar cell.<sup>[12]</sup> Considering the modification method herein, Nd was doped in  $\text{TiO}_2$  rods so that there was little likelihood to form a thin layer of  $\text{Nd}_2\text{O}_3$  on the surface of the electrode. Therefore, the photovoltage of the modified solar cell did not show obvious improvement.

As the  $\text{Nd}^{3+}$  ions were doped in the  $\text{TiO}_2$  nanorods, the doping would introduce electron states into the band gap of  $\text{TiO}_2$  and narrow the band gap.<sup>[23]</sup> From this point, the ions would probably feature as intraband-gap states<sup>[24]</sup> or surface

states<sup>[25]</sup> on the surface of the  $\text{TiO}_2$ . It is known that these states are usually recombination sites for injected electrons.<sup>[24,25]</sup> In DSSCs, they decrease the short-circuit current. On the other hand, Willner and co-workers<sup>[26]</sup> reported that lanthanide ions form complexes with various Lewis bases, including acids, amines, aldehydes, alcohols, and thiols, through the interaction of the functional groups with their fully or partially empty 4f orbitals. In the photocatalytic degradation of salicylic acid and *trans*-cinnamic acid by undoped and lanthanide oxide doped  $\text{TiO}_2$  nanoparticles, the enhanced degradation is attributed to the formation of the Lewis acid–base complex between the lanthanide ion and the substrates at the photocatalyst surface.<sup>[26]</sup> In the case of complexation between N719 and Nd ions or Ti ions, N719 bearing four carboxy groups (structure in Figure 3) acted as a Lewis acid, whereas the Nd and Ti ions acted as Lewis bases. Because of their 4f electrons, the Nd ions are more basic than the Ti ions. As a result, the coupling of N719 with Nd ions is stronger than with Ti ions. This strong coupling facilitates the transport of excited electrons.<sup>[27]</sup> We therefore suggest that Nd ions doped in the nanorods enhance the injection of excited electrons and simultaneously decrease the recombination rate of the injected electrons to improve the short-circuit photocurrent. Hence, the doped Nd ions play two different roles in the DSSC: one as a surface state and another as a coupling site. The former role is unfavorable, whereas the latter is favorable for a DSSC. The experimental results show that the latter effect compensated for and dominated over the former, thus increasing the short-circuit photocurrent of the modified electrode.

Furthermore, longer particles such as nanorods, nanowires, or nanotubes are constructed of isoelectronic materials that permit easy electron transport along the length of the particle.<sup>[28]</sup> When nanorods were used instead of nanoparticles, the number of contact barriers between titania material decreased. As the contact barriers usually act as electron traps, the total series resistance of DSSCs based on nanoparticles was higher than that of DSSC based on nanorods.<sup>[28]</sup> The fill factor has a close relationship with the total series resistance of a cell. When the electrons can quickly transport through the  $\text{TiO}_2$  film to the substrate without large resistance, the value of the fill factor increases, otherwise, the value decreases.<sup>[29]</sup> In this study, nanorods were used to modify the nanoparticle film, so that after modification a certain quantity of nanorods is present in the electrode film. Accordingly, the fill factor of the modified solar cell is enhanced. As analyzed earlier, the majority of the rods were embedded in the porous electrode. We could not exclude the possibility that some of the rods would be embedded parallel to the substrate. However, other embedded rods not parallel to the substrate would either supply a relatively short route to the substrate or, to a certain degree, confine the transport direction of the injected electrons and sweep them to the substrate. From the analyses made above, nanorods play two roles in DSSCs: one decreases the total series resistance of the cell, hence increasing the fill factor of the cell; the other accelerates the transport rate of the in-

jected electrons, hence improving the collection rate of the injected electrons.

## Conclusions

Nd-doped TiO<sub>2</sub> nanorods were synthesized and, for the first time, used to modify the conventional TiO<sub>2</sub> electrode in DSSCs. The modification remarkably enhanced the short-circuit photocurrent and the fill factor, thus leading to a 33.3% increase in power conversion efficiency. Our study indicates that the incorporation of Nd-doped TiO<sub>2</sub> nanorods into randomly assembled mesoporous films is a novel strategy to modify the photoanode in DSSCs. Such nanorods were easily embedded, did not affect the adsorption amount of dye sensitizer, and gave higher energy-conversion efficiency. The mechanism is likely to be that Nd ions doped on TiO<sub>2</sub> nanorods to some extent enhance the injection of excited electrons and decrease the recombination rate of the injected electrons. The introduction of rods not only decreases the total series resistance of a cell (hence increasing the fill factor of the cell) but also accelerates the transport rate of the injected electrons, hence improving the collection rate of injected electrons.

## Experimental Section

Monodispersed Nd-doped TiO<sub>2</sub> nanorods were synthesized according to the literature.<sup>[20,21]</sup> For example, oleic acid (7 mL), triethylamine (5 mL), and cyclohexane (20 mL) were mixed by stirring to form a transparent solution. Ti(OBu)<sub>4</sub> (1 mL) was added dropwise to the solution. Neodymium nitrate ( $\approx 5$  atom %, i.e., the molar ratio of Nd<sup>3+</sup> to Ti<sup>4+</sup> is 1:20) was then added to the mixed solution. After stirring at room temperature for a further 5 min, the solution was transferred into a teflon-lined stainless-steel autoclave at 180 °C for 1 day. Detailed procedures for preparing nanocrystalline TiO<sub>2</sub> films have been described in the literature.<sup>[3,22]</sup> The glass substrate used in this paper was indium tin oxide (ITO) (with a sheet resistance of 15  $\Omega$ /square, China Southern Glass Holding Co. Ltd), and the thickness of TiO<sub>2</sub> film used in this work was  $\approx 5$   $\mu$ m. The surface-modified TiO<sub>2</sub> electrode was fabricated by dipping a TiO<sub>2</sub> thin film into a solution of Nd-doped TiO<sub>2</sub> nanorods in cyclohexane (typical concentration of 2%) for 30 min, washed thoroughly with cyclohexane, dried, and sintered at 450 °C in air for 30 min. The fabrication of the solar cell was the same as documented in the literature.<sup>[22]</sup> Photoelectrochemical experiments were carried out with a standard two-electrode system.<sup>[21]</sup> Photocurrent–voltage (*I*–*V*) curves were measured with a Keithley 2410 SourceMeter under illumination from a 500-W Xe lamp, whose intensity was measured with a radiometer (FZ-A, Beijing Normal University, China). Monochromatic light in the range 400–800 nm was obtained by setting a WDG10 monochromator (Beijing Optical Instrument Factory, China) before the solar cell. The effective area is 0.196 cm<sup>2</sup>, and the redox electrolyte solution was composed of LiI (0.5 mol dm<sup>-3</sup>), I<sub>2</sub> (0.05 mol dm<sup>-3</sup>), and 4-*tert*-butylpyridine (0.5 mol dm<sup>-3</sup>) in 3-methoxypropionitrile.

XRD was performed on a Bruker D8 Advance X-ray diffractometer with Cu<sub>K $\alpha$</sub>  radiation ( $X = 1.5418$  Å). The  $2\theta$  range used was 20°–70° in steps of 0.02° with a count time of 1 s. The size and morphology of the nanorods were measured with a Hitachi Model H-800 transmission electron microscope, and the surface morphology of the electrodes was characterized with a LEO 1530 scanning electron microscope. Absorption measurements were made with a Hitachi mode U-3010 spectrophotometer.

## Acknowledgements

This work was supported by the NSFC, the Foundation for the Author of National Excellent Doctoral of P. R. China, and the State Key Project of Fundamental Research for Nanomaterials and Nanostructures.

- [1] M. Grätzel, *Nature* **2001**, *414*, 338–344.
- [2] M. K. Nazeeruddin, P. Péchy, T. Renouard, S. M. Zakeeruddin, R. Humphry-Baker, P. Comte, P. Liska, L. Cervery, E. Costa, V. Shlover, L. Spiccia, G. B. Deacon, C. A. Bignozzi, M. Grätzel, *J. Am. Chem. Soc.* **2001**, *123*, 1613–1624.
- [3] C. J. Barbé, F. Arendse, P. Comte, M. Jirosek, F. Lenzmann, V. Shklover, M. Grätzel, *J. Am. Ceram. Soc.* **1997**, *80*, 3157–3171.
- [4] M. Grätzel, *Prog. Photovoltaics* **2000**, *8*, 171–185.
- [5] M. Zúkalová, A. Zúkal, L. Kavan, M. K. Nazeeruddin, P. Liska, M. Grätzel, *Nano Lett.* **2005**, *5*, 1789–1792.
- [6] K. Hou, B. Z. Tian, F. Y. Li, Z. Q. Bian, D. Y. Zhao, C. H. Huang, *J. Mater. Chem.* **2005**, *15*, 2414–2420.
- [7] M. Law, L. E. Greene, J. C. Johnson, R. Saykally, P. Yang, *Nat. Mater.* **2005**, *4*, 455–459.
- [8] Z. S. Wang, C. H. Huang, Y. Y. Huang, Y. J. Hou, P. H. Xie, B. W. Zhang, H. M. Cheng, *Chem. Mater.* **2001**, *13*, 678–682.
- [9] N. G. Park, M. G. Kang, K. M. Kim, K. S. Ryyu, S. H. Chang, D. K. Kim, J. V. D. Lagemaat, K. D. Benkstein, A. J. Frank, *Langmuir* **2004**, *20*, 4246–4253.
- [10] S. M. Yang, Y. Y. Huang, C. H. Huang, X. S. Zhao, *Chem. Mater.* **2002**, *14*, 1500–1504.
- [11] A. Zaban, S. G. Chen, S. Chappel, B. A. Gregg, *Chem. Commun.* **2000**, 2231–2232.
- [12] S. G. Chen, S. Chappel, Y. Diamant, A. Zaban, *Chem. Mater.* **2001**, *13*, 4629–4634.
- [13] E. Palomare, J. N. Clifford, S. A. Haque, T. Lutz, J. R. Durrant, *Chem. Commun.* **2002**, 1464–1465.
- [14] E. Palomare, J. N. Clifford, S. A. Haque, T. Lutz, J. R. Durrant, *J. Am. Chem. Soc.* **2003**, *125*, 475–482.
- [15] B. C. O'Regan, S. Scully, A. C. Mayer, E. Palomares, J. Durrant, *J. Phys. Chem. B* **2005**, *109*, 4616–4623.
- [16] H. S. Jung, J. Lee, M. Nastasi, S. Lee, J. Kim, J. Park, K. S. Hong, H. Shin, *Langmuir* **2005**, *21*, 10332–10335.
- [17] Y. Diamant, S. G. Chen, O. Melamed, A. Zaban, *J. Phys. Chem. B* **2003**, *107*, 1977–1981.
- [18] N. Okada, S. Karuppachamy, M. Kurihara, *Chem. Lett.* **2005**, 16–17.
- [19] S. M. Yang, F. Y. Li, C. H. Huang, *Sci. China Ser. B* **2003**, *1*, 59–65.
- [20] X. Wang, J. Zhuang, Q. Peng, Y. D. Li, *Nature* **2005**, *437*, 121–124.
- [21] X. L. Li, Q. Peng, J. X. Yi, X. Wang, Y. D. Li, *Chem. Eur. J.* **2006**, *12*, 2383–2391.
- [22] Z. Wang, F. Li, C. Huang, L. Wang, M. Wei, L. Jin, N. Li, *J. Phys. Chem. B* **2000**, *104*, 9676–9682.
- [23] W. Li, Y. Wang, H. Lin, S. Ismat Shaha, C. P. Huang, D. J. Doren, S. A. Rykov, J. G. Chen, M. A. Barteau, *Appl. Phys. Lett.* **2003**, *83*, 4143–4145.
- [24] J. Nelson, *Phys. Rev. B* **1999**, *59*, 15374–15380.
- [25] I. Mora-Seró, J. Bisquert, *Nano Lett.* **2003**, *3*, 945–949.
- [26] K. T. Ranjit, I. Willner, S. H. Bossmann, A. M. Braun, *J. Catal.* **2001**, *204*, 305–313.
- [27] S. Anderson, E. C. Constable, M. P. Dare-Edwards, J. B. Goode-nough, A. Hamnett, K. R. Seddon, R. D. Wright, *Nature* **1979**, *280*, 571–572.
- [28] M. S. Dresselhaus, Y. M. Lin, O. Rabin, A. Jorio, A. G. Souza Filho, M. A. Pimenta, R. Saito, G. Samsonidze, G. Dresselhaus, *Mater. Sci. Eng. C* **2003**, *23*, 129–140.
- [29] J. T. Jiu, S. Isoda, F. M. Wang, M. Adachi, *J. Phys. Chem. B* **2006**, *110*, 2087–2092.

Received: June 20, 2006

Published online: October 20, 2006